Nitric Oxide 92 (2019) 34–40

Contents lists available at ScienceDirect

Nitric Oxide

journal homepage: www.elsevier.com/locate/yniox

# Visible light-controlled NO generation for photoreceptor-mediated plant root growth regulation

Suprakash Biswas[a], Neha Upadhyay[b], Debojyoti Kar[b], Sourav Datta[b,**], Apurba Lal Koner[a,*]

[a] Department of Chemistry, Indian Institute of Science Education and Research Bhopal, Bhopal Bypass Road, Bhauri, Bhopal, Madhya Pradesh, India
[b] Department of Biological Sciences, Indian Institute of Science Education and Research Bhopal, Bhopal Bypass Road, Bhauri, Bhopal, Madhya Pradesh, India

A B S T R A C T

Nitric oxide (NO) is an essential redox-signaling molecule free radical, contributes a significant role in a diverse range of physiological processes. Photo-triggered NO donors have significant potential compared to other NO donors because it releases NO in the presence of light. Hence, an efficient visible light-triggered NO donor is designed and synthesized by coupling 2,6-dimethyl nitrobenzene moiety at the *peri*-position of 1, 8-naphthalimide. The NO-releasing ability is validated using various spectroscopic techniques, the photoproduct is characterized, and finally, the NO generation quantum yield is also determined. Furthermore, the photo-generated NO has been employed to *Arabidopsis thaliana* as a model plant to examine the effect of photoreceptor-mediated NO uptake on plant root growth regulation molecule.

## 1. Introduction

Nitrogen monoxide is considered one of the most important signaling agents, exists in three interrelated chemical forms including nitrosonium cation ($NO^+$), nitric oxide ($NO^•$), and nitroxyl anion ($NO^-$) [1,2]. Nitric oxide (NO) exists as a highly reactive free radical or reactive oxygen species (ROS), sometimes also referred to as reactive nitrogen species (RNS), and performs as an important multitasked-signaling agent in various biological processes [3–5]. NO has also been identified as an endothelium-derived relaxing factor (EDRF) in blood vessels, and the nitric oxide synthase is mainly responsible for NO production in living systems [6–8]. Besides, several diseases such as schizophrenia, Alzheimer's disease, and cancer are related to malfunction of NO signaling and its dynamics [9,10]. For the past few decades, researchers also found that NO performs a crucial role in plant growth regulations [11,12]. In the metabolism of inorganic nitrogenous compounds in higher plants and nitrogen-fixing organism, NO is generated as a pivotal intermediate [13]. Recent literature on plant biology reveals that NO influences primary root development through the initiation of cell-cycle genes and patterns of cellulose synthesis [14,15]. Additionally, being an essential signaling agent, deficiency of NO affects auxin biosynthesis, transport, and signaling pathways. The highly reactive nature of NO and its tremendous biological importance fascinated the researchers for *in-situ* generation of NO in biological systems [16]. For potential therapeutic applications in living systems, the NO-donors must release NO in a time-controlled and site-specific manner [17]. To date, numerous NO-donors such as 1-hydroxy-2-oxo-3-(aminoalkyl)-1-triazenes, 4-alkyl-2 hydroxyimino-5-nitro-3-hexenes, *etc*. are reported in the literature [18,19]. Among them, photo-triggered NO-donors secure extraordinary attention to the researchers due to the release of NO with high spatiotemporal control. Miyata group reported 6-Nitrobenzo[α] pyrene derivative that generates NO in the presence of visible light [20]. Later, they reported a series of NO-releasing molecules, comprising of a hindered nitrobenzene derivative, but all those molecules are poorly water-soluble [21]. However, the recently reported light-induced NO-donors suffer from excitation of ultraviolet and two-photon radiation [22–25]. Therefore, there is an urgent need of a visible-light triggered efficient NO-donor, which can generate NO in considerable time and dose-dependent manner.

In this contribution, we have designed and synthesized a naphthalene monoimide-based fluorescent molecule (**Ni–$NO_2$**) for a visible-light-induced NO generation. Highly photostable naphthalimide dyes helps to reduce the toxic effect of different photo-generated product, whereas other photo-unstable molecules might cause a toxic effect due to the formation of different photo-degraded product other than the desired NO. Thus, we have attached a sterically hindered nitrobenzene moiety, *i.e.*, 2, 6-dimethyl nitrobenzene, at the *peri*-position of 1, 8-naphthalimide ring through an alkene spacer. Subsequently, an elaborated spectroscopic investigation was performed to understand the visible light-triggered NO release in various solvent. We confirm the NO release from Ni–$NO_2$ by Griess assay, EPR spectroscopy and the photochemical quantum yield for the release of NO was also determined. After confirming the release of NO we have also characterized the photoproduct using mass spectrometry. Further, the NO-releasing

* Corresponding author.
** Corresponding author.
*E-mail addresses:* sdatta@iiserb.ac.in (S. Datta), akoner@iiserb.ac.in (A.L. Koner).

https://doi.org/10.1016/j.niox.2019.07.010
Received 28 May 2019; Received in revised form 29 July 2019; Accepted 31 July 2019
Available online 01 August 2019

molecule was employed to comprehend the effect of NO in photoreceptor-mediated plant root and root-hair growth regulation. Hence, to inspect the effect of NO released from **Ni–$NO_2$**, we used *Arabidopsis thaliana* as a model plant and the effect of its root growth as a functional assay under the various fluence of visible light. We found a considerable root growth inhibition of *Arabidopsis thaliana* with different photoreceptor.

## 2. Materials and methods

### 2.1. General materials and method

All the reactions were performed in oven-dried glassware under a nitrogen atmosphere where required and stirred with Teflon-coated magnetic stirring bars. Tetrahydrofuran was distilled over sodium/benzophenone ketyl. All other solvents and reagents were used as received unless otherwise stated. Reaction temperatures above room temperature (298 K) refer to oil bath temperature.

### 2.2. Methods

Thin layer chromatography was performed using Merck Silica gel 60 F-254 pre-coated plates and visualized using UV irradiation ($\lambda$ = 254/365 nm). Silica gel from Merck (particle size 100–200 mesh) was used for column chromatography. $^1$H and $^{13}$C NMR spectra were recorded on Bruker 400 MHz spectrometers with operating frequencies of 100 MHz for $^{13}$C. Chemical shifts ($\delta$) are reported in ppm relative to the residual solvent signal ($\delta$ = 7.26 for $^1$H NMR and $\delta$ = 77.0 for $^{13}$C NMR). High-resolution mass spectrometry (HRMS) data were recorded on MicrOTOF-Q-II mass spectrometer using chloroform as the solvent. All the reagents and solvents were brought from sigma used without further purification. Water used was of Milli-Q grade using a Millipore water purification system with resistivity 18.2 MΩ, for the phosphate buffer preparation. All absorption spectra and fluorescence measurements were carried out using SHIMADZU spectrophotometer and HORIBA JobinYvon fluorimeter (fluorolog) using 1 cm path length quartz cuvettes. EPR spectra measurement was carried out in BRUKER A-300, X-band EPR spectrometer with modulation amplitude of 3 G, modulation frequency 10 KHz, and central field 3440 G. HPLC experiments were performed using a UV detector from Waters 2489 fitted with a reverse-phase C18 column 5 mm, 4.6 mm × 250 mm. Samples were injected using a auto-sampler from Waters (part no: 2707). NMR spectroscopic characterization was taken on a BRUKER Advance 400 MHz spectrometer. A 2.0 mM stock solution of **Ni–$NO_2$** was prepared in DMSO and then further diluted to 1.0 μM in phosphate buffer of pH 6.0 to check the absorption and steady-state fluorescence spectra of **Ni–$NO_2$**.

### 2.3. Theoretical calculation

Density functional theory calculations were performed on **Ni–$NO_2$** using Gaussian 09 suite of quantum chemical programs [26]. Ground-state geometry optimizations were performed with Becke three-parameter exchange functional in conjunction with Lee-Yang-Parr correlation functional (B3LYP) [27–29] using 6-311G as a basis set.

### 2.4. Plant materials and growth conditions

*Arabidopsis thaliana* Columbia-0 (Col-0) ecotype, *phyB-9*, *cry1cry2* seeds were used in this study. Seeds were surface-sterilized with 5% (v/v) bleach solution for about 3 min, rinsed with sterile water at least four times, and then sown on half-strength Murashige and Skoog (1/2 MS) medium containing 0.8% (w/v) agar. After 3 d at 4 °C in the dark to synchronize germination, the plates were transferred to a growth chamber with continuous white light (about 110 $\mu$M $m^{-2}$ $s^{-1}$) and maintained at 22 °C for 5 days. To avoid possible effects of chemicals other than NO gas on root growth, NO treatments were performed by photochemical release of NO gas from the NO donor **Ni–$NO_2$** and sodium nitroprusside (SNP), which was mixed with a small amount of growth medium before solidification and added inside the upper cover of the plates at the desired concentrations. Seedlings grew on **Ni–$NO_2$** and SNP-free agar medium in the lower portion of the plate. In this way, we could ensure that the effect on the seedlings was due to NO rather than to **Ni–$NO_2$** and SNP.

### 2.5. Root length measurement

Seedlings were laid horizontally on the agar plates, digital pictures were taken, and primary root length and root hair length of at least 30 seedlings were measured using ImageJ software.

## 3. Result and discussion

The design strategy of **Ni–$NO_2$** is based on photo-isomerization of the nitro group of the sterically-hindered nitrobenzene moiety, connected to the naphthalimide ring. Considering the photo-isomerization possibility, we have synthesized **Ni–$NO_2$** according to the above synthetic scheme (Scheme 1, for the detail, see Scheme S1).

Density functional calculation reveals that the nitro group is in non co-planar conformation with a twist angle of *ca.* 42°, with respect to the benzene ring due to the steric hindrance of two *ortho*-methyl groups (Schemes S2a–b and Fig. S1). Upon photo-irradiation, the twisted nitro group rearranges and isomerizes to nitrite ester [22], owing to the generation of NO.

After the synthesis and characterization, we validated the optical purity by comparing UV–Vis. and excitation spectra in phosphate buffer (PB, pH 6, Fig. 1a). **Ni–$NO_2$** has an absorption maximum in PB at around 400 nm, whereas it emits around 517 nm (Fig. 1a) with a large Stokes shift of 117 nm. To understand the swiftness of NO-releasing properties of **Ni–$NO_2$**, we have kinetically monitored its fluorescence properties under visible-light excitation (113 Lux) in 1 mM PB at pH 6. The fluorescence intensity of **Ni–$NO_2$** gets attenuated upon visible-light mediated excited-state isomerization of the nitro group. Interestingly, within 20 min of irradiation, we have obtained a plateau in the emission intensity indicating completion of NO release (Fig. 1b). The

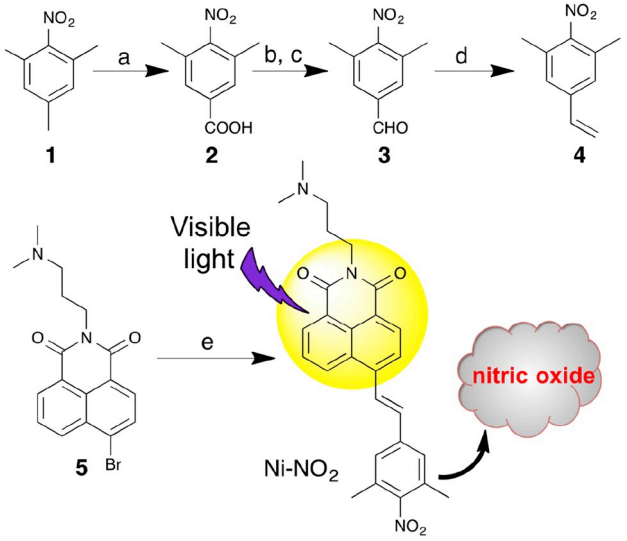


(a) $CrO_3$, glacial AcOH, RT, 10 h, 34%; (b) $NaBH_4$, $F_3B$-$OEt_2$, dry THF, RT, 8 h, 67%; (c) $MnO_2$, dry DCM, Reflux, 6 h, 74%; (d) $K_2CO_3$, dry THF, $Ph_3\overset{\oplus}{P}$-$CH_3\overset{\ominus}{I}$, Reflux, 24 h, 80%; (e) **4**, $Pd(OAc)_2$, P(*o*-tol)$_3$, ACN-$Et_3N$, Reflux, 24 h, 44%.

**Scheme 1.** Synthesis of **Ni–$NO_2$** for visible-light mediated nitric oxide generation.

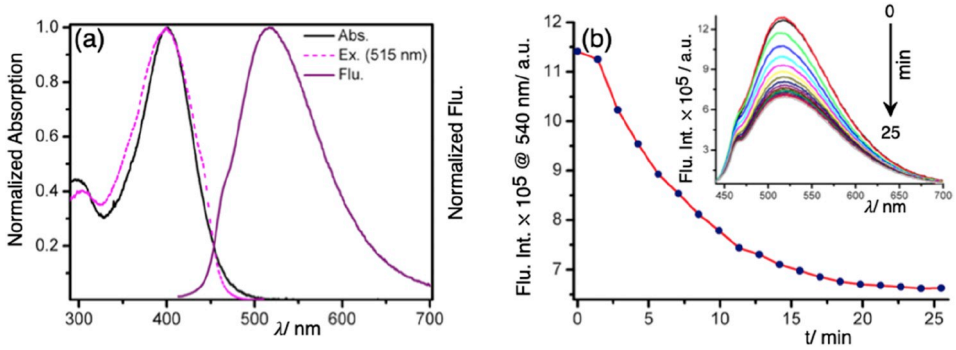


**Fig. 1.** (a) The absorption, excitation, and emission spectra of **Ni–NO$_2$** in PB at pH 6.0, (b) kinetic monitoring of fluorescence intensity of 1 $\mu$M **Ni–NO$_2$** at 540 nm in PB upon excitation of 410 nm light at 298 K; inset shows fluorescence spectra of the same at different time interval.

fluorescence attenuation is possibly due to the formation of the phenolic group and its interaction with the solvent [30]. Further, to verify the effect of light intensity on the NO release rate, we have performed kinetic monitoring of NO release experiment using a neutral density filter and recorded the emission spectra of **Ni–NO$_2$**. As expected, we obtained a plateau after 30 min (Figs. S2–3) confirming the role of light intensity for NO release. Furthermore, we have performed a modified Griess assay to validate NO generation through the photolysis of **Ni–NO$_2$**. The photo-induced production of NO was verified by the detection of $NO_2^-$, arising from the auto-oxidation of NO in PB medium [31]. The appearance of a red color solution having absorption at 542 nm supports the diazo-coupling reaction of $NO_2^-$ with the Griess reagents (GR, Scheme S3). To perform this assay, we have taken 50–150 $\mu$M of **Ni–NO$_2$** in $CHCl_3$ and excited by 410 nm light for ~50 min, and then the mixture was allowed to react with GR. Finally, the absorption spectrum of the red color solution was measured. The increase optical density at 542 nm upon increasing concentration of **Ni–NO$_2$**, signifies the successful generation of NO (Fig. 2a). Further, to verify the photo-triggered generation of NO, an EPR experiment was also performed using 2-phenyl-4, 4, 5, 5,-tetramethylimidazoline-1-

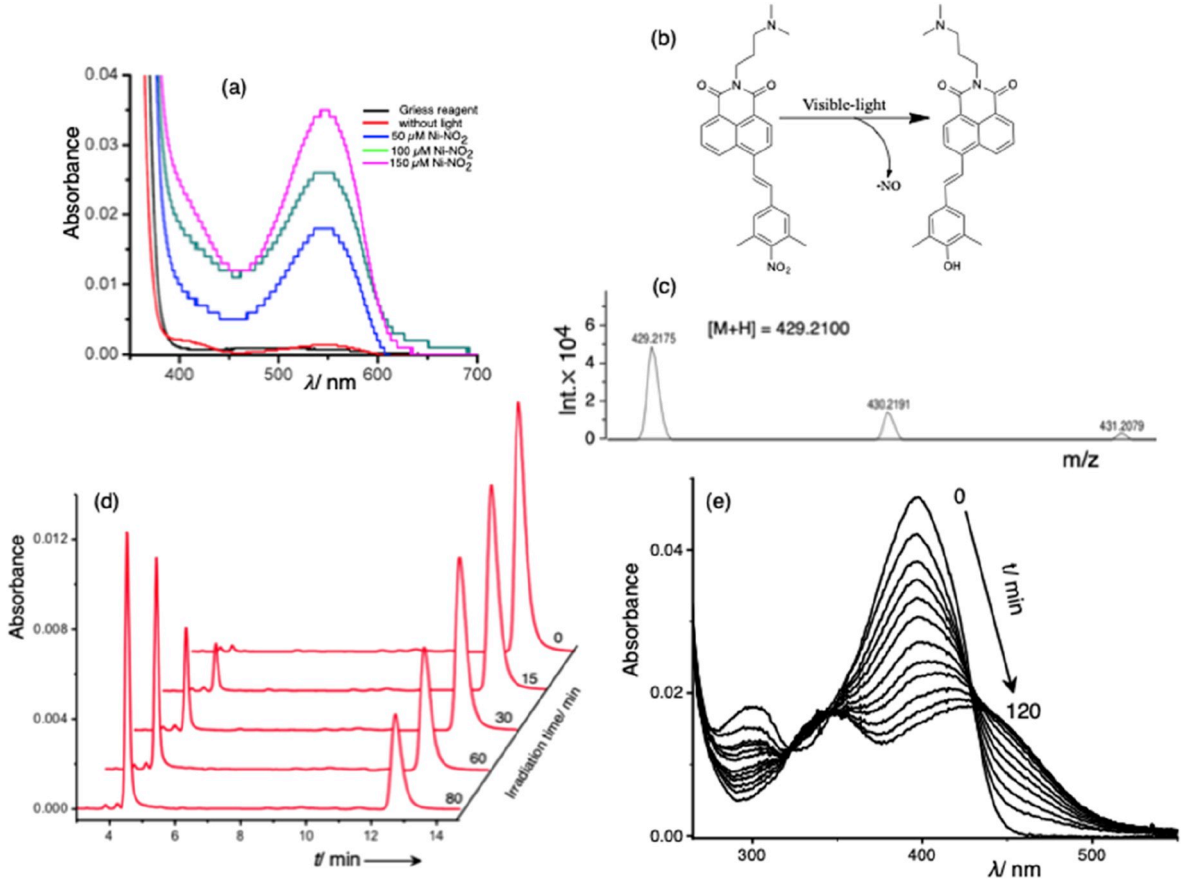


**Fig. 2.** (a) Absorption spectra of the reaction between Griess solution with a photo-irradiated **Ni–NO$_2$** solution, (b) chemical structure of the photo-generated product of **Ni–NO$_2$** and (c) the mass-spectrum of the product after photodecomposition, (d) the HPLC profile of photo-triggered NO generation experiments and (e) time-dependent absorption spectra of **Ni–NO$_2$** (2 $\mu$M) in DMSO upon photo-irradiation using white light.

oxyl-3-oxide (PTIO) as a spin trap for NO [23].

PTIO is a stable radical shows characteristic five lines in the EPR spectrum, and it oxidizes NO to $NO_2$ and converted to 2-phenyl-4,4,5,5, tetramethylimidazoline- 1-oxyl (PTI) which is also a persistence radical. Hence, there will be a significant change in the EPR signal due to the formation of PTI, signifies the formation of NO. After the photo-irradiation of a mixture of PTIO and **Ni–$NO_2$** for 30 min with white light the EPR spectrum was recorded. The characteristic change of EPR spectrum compared to PTIO further confirms the generation of NO from **Ni–$NO_2$** (Fig. S4).

Additionally, we have performed a HPLC experiment to monitor the progress of the reaction. For the HPLC measurement, we have irradiated 10 $\mu$M of **Ni–$NO_2$** in acetonitrile using 390 nm light at 0, 15, 30, 60, and 80 min interval (see Figs. 2b and SI for details). A linear decrease in the absorption intensity corresponding to the reactant having an elution time 12.8 min and subsequent increase in the absorption intensity for the product at an elution time of 4.6 min were observed (Fig. 2b). The photodecomposition quantum yield of NO release was measured as *ca.* 0.036 in acetonitrile (for details see SI, Figs. S5–7). Such low photodecomposition quantum yield of NO is due to the competitive *cis-trans* isomerization pathway responsible for such molecules [32]. The photo-degraded product was also identified by mass spectrometry (Fig. 2c and d). Further, the photo-reaction was also monitored by absorption spectroscopy in different time interval in DMSO (Fig. 2e) and in other solvents (see Fig. S8). The absorption spectra in DMSO reveal a decrease in the absorption maxima at 400 nm with the generation of a new absorption peak at around 427 nm, which also confirms the formation of the expected photo-generated product [30].

After the spectroscopic characterization of the NO release in the presence of visible-light, we have investigated the effect of NO on plant roots and root-hair growth. A thorough literature survey suggests that NO inhibits root growth in a dose-dependent manner [33]. Hence, to determine the effect of NO released from **Ni–$NO_2$**, we used *Arabidopsis thaliana* as a model plant and its root growth inhibition as a functional assay. Arabidopsis seeds (Col-0 ecotype) were inoculated on growth medium supplied with 0, 0.2, 1.0, 5.0, 10.0, 30.0 $\mu$M of **Ni–$NO_2$**. The NO-donor **Ni–$NO_2$** was added inside the upper cover of plates at desired concentrations (Fig. S9). Seedlings were grown on **Ni–$NO_2$** free agar medium in the lower portion of the plate to avoid side effects of NO-donor reagents [34]. One set of plates was kept under cycling white light (WL, 110 $\mu$M $m^{-2}$ $sec^{-1}$) while the other set was kept under darkness. After six days, seedlings grown under light and containing **Ni–$NO_2$** in the upper lid showed significantly reduced primary root length as compared to the plate without **Ni–$NO_2$** (Fig. 3a).

On the other hand, seedlings grown in the dark did not exhibit any significant difference in root length in presence or absence of the **Ni–$NO_2$** (Fig. 3a). These results suggest that the photo-activation of **Ni–$NO_2$** promotes the release of NO that causes root growth inhibition in plants. In order to evaluate the efficiency of **Ni–$NO_2$** derived NO on root growth inhibition, we used sodium nitroprusside (SNP), a well-established NO-donor, and compared the effects on primary root growth inhibition (Fig. 3b and c) [35]. At similar concentrations of these two NO-donors the root elongation defect was either comparable or more severe in **Ni–$NO_2$** compared to SNP. Further, we examined the effect of **Ni–$NO_2$** and SNP with varying fluence levels of cycling WL, 35, 85 and 150 $\mu$M $m^{-2}$ $sec^{-1}$ (Fig. 3b and Figs. S10a–b). At all fluence levels, both the NO-donors showed reduced primary root length in a

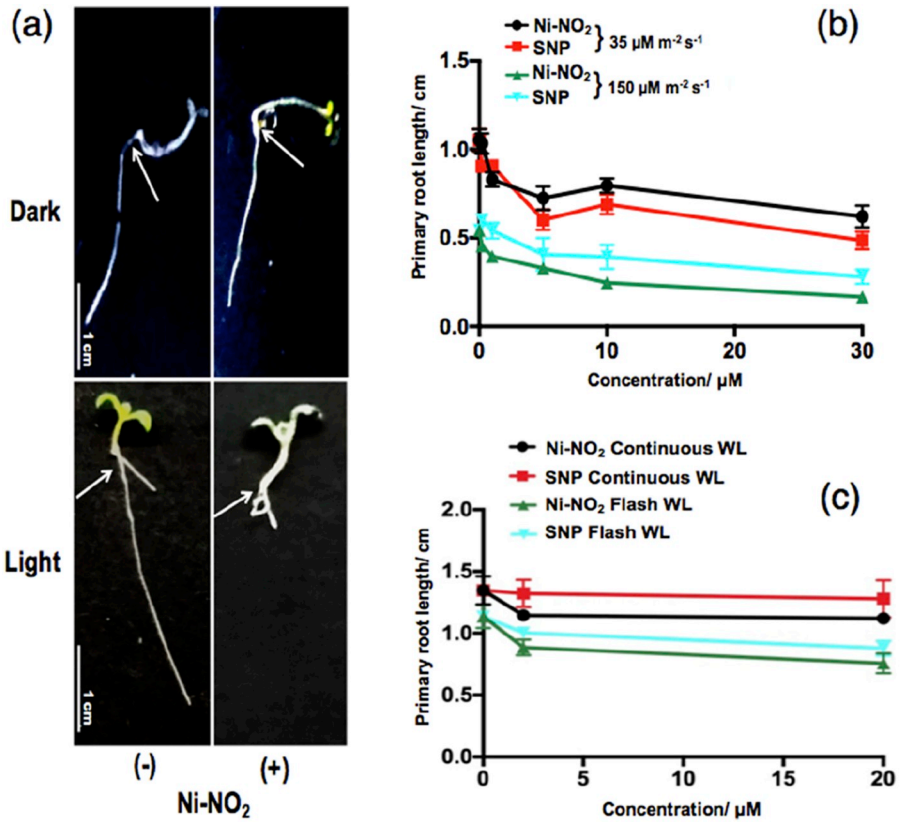


**Fig. 3.** The response of Arabidopsis (Col-0) roots to **Ni–$NO_2$** under dark and light. (a) 6 days old seedlings grown on MS media plates supplemented with 0, 10 $\mu$M **Ni–$NO_2$** in continuous dark and cycling WL at 110 $\mu$M $m^{-2}$ $s^{-1}$ fluence level. Part of seedling below white arrow shown in (a) indicates root that is inhibited by **Ni–$NO_2$** in light due to the release of NO. (b) Primary root length of Col-0 seedlings treated with 0, 0.2, 1, 5, 10, 30 $\mu$M of **Ni–$NO_2$** and SNP at two different fluence levels 35 and 150 $\mu$M $m^{-2}$ $s^{-1}$ of cycling WL (c) and in continuous WL (110 $\mu$M $m^{-2}$ $s^{-1}$) and flash of WL (110 $\mu$M $m^{-2}$ $s^{-1}$ for 1 h). Scale bar, 1 cm in (a).

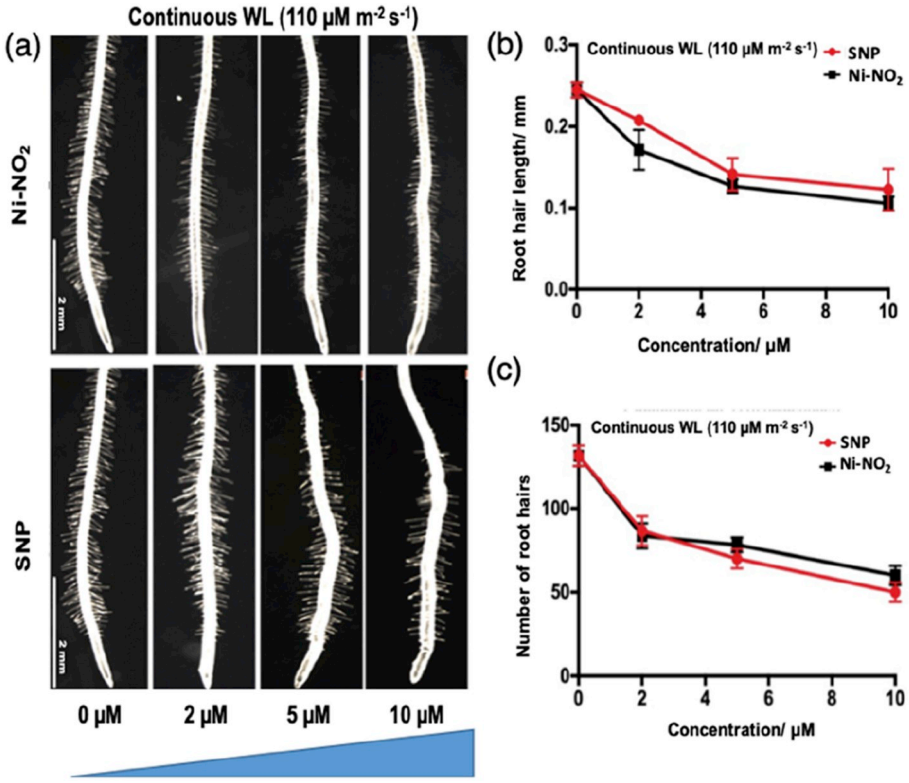


**Fig. 4.** Inhibition of root hair development by **Ni–$NO_2$** under WL. (a) Root hair image of 6 days old Col-0 seedlings grown on medium supplemented with 0, 2, 5, 10 $\mu$M **Ni–$NO_2$** and SNP in continuous WL at 110 $\mu$M $m^{-2}$ $s^{-1}$ fluence level (b) Root hair length measurement of Col-0 seedlings treated as described in (a). (c) Root hair number measurement of Col-0 seedlings treated as described in (a). Mean values and S.E. were calculated from at least 30 seedlings. Scale bar, 2 mm in (a).

dose-dependent manner. We also determined the effect of continuous WL and flash of WL (1 h at 150 $\mu$M $m^{-2}$ $sec^{-1}$) on NO-donors by using different doses of **Ni–$NO_2$** and SNP (0, 2 and 20 $\mu$M) and exposing them to continuous or flash of WL. Both the light conditions exhibited an inhibitory effect on primary root growth (Fig. 3c and Figs. S11a and S12a). Further, we investigated the effect of monochromatic blue light (BL) on NO-donors by exposing plants to continuous BL (150 $\mu$M $m^{-2}$ $sec^{-1}$) and a flash of BL (1 h at 150 $\mu$M $m^{-2}$ $sec^{-1}$, see SI). Both **Ni–$NO_2$** and SNP markedly inhibited primary root length under continuous BL (SI, Figs. S11b and S12b). Under flash of BL, **Ni–$NO_2$** at 2 $\mu$M concentration promoted primary root length while at 20 $\mu$M concentration it showed an inhibitory effect on root growth (Figs. S12b and S13b). This might be due to cell elongation effect at a low concentration of NO under BL [36]. We also examined the effect of different concentrations (0–10 $\mu$M) of **Ni–$NO_2$** and SNP on root-hair growth when exposed to continuous WL (110 $\mu$M $m^{-2}$ $sec^{-1}$). Root hair growth is inhibited (reduced root hair length and number) in a dose-dependent manner (Fig. 4a–c). This result suggests that the regulatory effect of **Ni–$NO_2$** on root growth of Arabidopsis seedlings is light dependent. Upon exposure to light, the photolysis of **Ni–$NO_2$** releases NO, which inhibits root growth.

Light-mediated release of NO also activates various photoreceptors in plants. Phytochrome (PHY) and cryptochrome (CRY), red and BL receptors respectively are reported to be NO-responsive. NO release causes nuclear accumulation of *phyB-9* which positively regulates primary root growth inhibition [34]. To verify, if the NO-induced primary root growth inhibition is photoreceptor mediated, we quantified root length in the photoreceptor mutants *phyB-9* and *cry1cry2* (Fig. 5 and S14-18). Our results indicate that phyB-9 and *cry1cry2* exhibit hyposensitivity to the NO released by 2 $\mu$M **Ni–$NO_2$**. At 10 $\mu$M concentration of **Ni–$NO_2$** the root growth inhibition was also observed in the mutants, especially under WL possibly due to the activation of other photoreceptors in the single mutant (Fig. 5). Under the monochromatic BL condition, *cry1cry2* double mutant display almost insensitivity at a higher concentration indicating that NO-induced primary root growth inhibition is photoreceptor mediated (Fig. 5c and d).

## 4. Conclusion

In conclusion, we have designed and developed a naphthalene monoimide-based fluorescent NO-donor **Ni–$NO_2$** by attaching 2,6 dimethyl nitrobenzene at the *peri*-position of 1,8-naphthalimide ring through an alkene bond. The synthesized molecule releases NO upon photoexcitation with visible light and the NO generation was confirmed by Griess assay, EPR spin trapping, high-resolution mass spectrometry, and optical spectroscopic investigations in various solvents. Further, the progress of the reaction was monitored using HPLC. The photodecomposition quantum yield of **Ni–$NO_2$** in acetonitrile was also determined. The fluorescence intensity of the probe gets attenuated by releasing NO in aqueous solution and its get saturated within 20 min signifying the rapid release of NO. Finally, the released NO was employed for Arabidopsis root growth assay either by continuous or flash of white and blue light irradiation. Our results indicate NO-mediated regulation of primary root and root hair growth by **Ni–$NO_2$** in a photoreceptor mediated manner. These findings can potentially open up prospects for generation of an effective weedicide in the future.

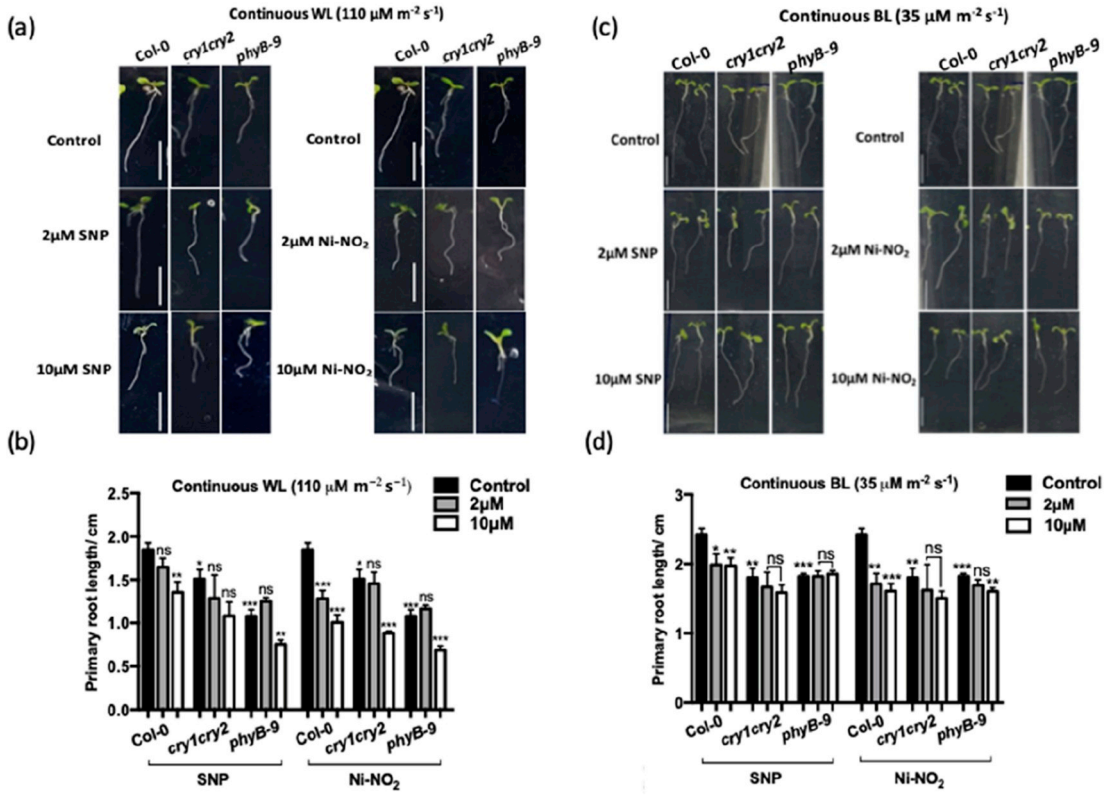


**Fig. 5.** Response of WT, *cry1cry2* and *phyB-9* mutants to NO under continuous WL and BL (a) WT, *cry1cry2* and *phyB-9* seedlings growing on medium supplemented with SNP and **Ni–NO$_2$** at various concentration under WL at 110 $\mu$M m$^{-2}$ s$^{-1}$ fluence. (b) Root length of WT, *cry1cry2* and *phyB-9* seedlings treated as in (a). (c) WT, *cry1cry2* and *phyB-9* seedlings growing on medium supplemented with SNP and **Ni–NO$_2$** at 0, 2 and 10 $\mu$M under BL at 35 $\mu$M m$^{-2}$ s$^{-1}$ fluence. (d) Root length of WT, *cry1cry2* and *phyB-9* seedlings treated as in (c). Mean value and SE were calculated from at least 20 seedlings. Significant difference was analyzed student's t-test with Welch's corrections compared to WT under same condition are indicated by asterisks: *P < .05, **P < .01, ***P < .001.

## Acknowledgements

We acknowledge the financial support from Indian Institute of Science Education and Research Bhopal (IISERB), India (INGRANT/CHM/2012017 for ALK) and central instrumentation facility (CIF) at IISERB. SB thanks University Grants Commission, India for his fellowship. SD would like to thank Department of Biotechnology (DBT), India (Ramalingaswami Fellowship, IYBA) and Science and Engineering Research Board (EMR/2016/000181), India for funding. NU and DK acknowledge Ministry of Human Resource Development and DBT (BT/PR19193/BPA/118/195/2016), India for fellowship. Authors acknowledge help of Mr. Anil Raj Narooka with HPLC measurements.

## Appendix A. Supplementary data

Supplementary data to this article can be found online at https://doi.org/10.1016/j.niox.2019.07.010.

## References

[1] M.N. Hughes, Biochim. Biophys. Acta 1411 (1999) 263–272.
[2] J.S. Stamler, D.J. Singel, J. Loscalzo, Science 258 (1992) 1898.
[3] P. Domingos, Ana M. Prado, A. Wong, C. Gehring, Jose A. Feijo, Mol. Plant 8 (2015) 506–520.
[4] J.S. Stamler, Cell 78 (1994) 931–936.
[5] S.K. Singh, S.M. Husain, ChemBioChem 19 (2018) 1657–1663.
[6] U. Förstermann, W.C. Sessa, Eur. Heart J. 33 (2012) 829–837.
[7] Y. Xia, J.L. Zweier, Proc. Natl. Acad. Sci. U.S.A. 94 (1997) 12705–12710.
[8] W.K. Alderton, C.E. Cooper, R.G. Knowles, Biochem. J. 357 (2001) 593.
[9] F.-Y. Huang, O.-O. Chan Annie, A. Rashid, K.-H. Wong Danny, C.-H. Cho, M.-F. Yuen, Cancer 118 (2012) 4969–4980.
[10] H.-J. Xiang, L. An, W.-W. Tang, S.-P. Yang, J.-G. Liu, Chem. Commun. 51 (2015) 2555–2558.
[11] S. Mangano, S.P.D. Juárez, J.M. Estevez, Plant Physiol. 171 (2016) 1593–1605.
[12] P. Domingos, Ana M. Prado, A. Wong, C. Gehring, Jose A. Feijo, Mol. Plant 8 (2015) 506–520.
[13] C.A. Fewson, D.J.D. Nicholas, Nature 188 (1960) 794–796.
[14] N. Correa-Aragunde, M. Graziano, C. Chevalier, L. Lamattina, J. Exp. Bot. 57 (2006) 581–588.
[15] N. Correa-Aragunde, C. Lombardo, L. Lamattina, New Phytol. 179 (2008) 386–396.
[16] J.A. McCleverty, Chem. Rev. 104 (2004) 403–418.
[17] S. Diring, D.O. Wang, C. Kim, M. Kondo, Y. Chen, S. Kitagawa, K.-i. Kamei, S. Furukawa, Nat. Commun. 4 (2013) 2684.
[18] K.M. Davies, D.A. Wink, J.E. Saavedra, L.K. Keefer, J. Am. Chem. Soc. 123 (2001) 5473–5481.
[19] C. Napoli, L.J. Ignarro, Annu. Rev. Pharmacol. Toxicol. 43 (2003) 97–123.
[20] K. Fukuhara, M. Kurihara, N. Miyata, J. Am. Chem. Soc. 123 (2001) 8662–8666.
[21] T. Suzuki, O. Nagae, Y. Kato, H. Nakagawa, K. Fukuhara, N. Miyata, J. Am. Chem. Soc. 127 (2005) 11720–11726.
[22] K. Kitamura, M. Kawaguchi, N. Ieda, N. Miyata, H. Nakagawa, ACS Chem. Biol. 11 (2016) 1271–1278.
[23] Z. Zhang, J. Wu, Z. Shang, C. Wang, J. Cheng, X. Qian, Y. Xiao, Z. Xu, Y. Yang, Anal. Chem. 88 (2016) 7274–7280.
[24] X. Xie, J. Fan, M. Liang, Y. Li, X. Jiao, X. Wang, B. Tang, Chem. Commun. 53 (2017) 11941–11944.
[25] K. Matsuo, H. Nakagawa, Y. Adachi, E. Kameda, H. Tsumoto, T. Suzuki, N. Miyata, Chem. Commun. 46 (2010) 3788–3790.
[26] M.J. Frisch, G.W. Trucks, H.B. Schlegel, G.E. Scuseria, M.A. Robb, J.R. Cheeseman, G. Scalmani, V. Barone, B. Mennucci, G.A. Petersson, H. Nakatsuji, M. Caricato, X. Li, H.P. Hratchian, A.F. Izmaylov, J. Bloino, G. Zheng, J.L. Sonnenberg, M. Hada, M. Ehara, K. Toyota, R. Fukuda, J. Hasegawa, M. Ishida, T. Nakajima, Y. Honda, O. Kitao, H. Nakai, T. Vreven, J.A. Montgomery Jr., J.E. Peralta, F. Ogliaro, M.J. Bearpark, J. Heyd, E.N. Brothers, K.N. Kudin, V.N. Staroverov, R. Kobayashi, J. Normand, K. Raghavachari, A.P. Rendell, J.C. Burant, S.S. Iyengar, J. Tomasi, M. Cossi, N. Rega, N.J. Millam, M. Klene, J.E. Knox, J.B. Cross, V. Bakken, C. Adamo, J. Jaramillo, R. Gomperts, R.E. Stratmann, O. Yazyev, A.J. Austin, R. Cammi, C. Pomelli, J.W. Ochterski, R.L. Martin, K. Morokuma, V.G. Zakrzewski, G.A. Voth, P. Salvador, J.J. Dannenberg, S. Dapprich, A.D. Daniels, O. Farkas, J.B. Foresman, J.V. Ortiz, J. Cioslowski, D.J. Fox, Wallingford, CT, U.S, 2009.
[27] C. Lee, W. Yang, R.G. Parr, Phys. Rev. B 37 (1988) 785–789.
[28] S.H. Vosko, L. Wilk, M. Nusair, Can. J. Phys. 58 (1980) 1200–1211.

[29] A.D. Becke, J. Chem. Phys. 98 (1993) 5648–5652.
[30] X. Zheng, W. Zhu, D. Liu, H. Ai, Y. Huang, Z. Lu, ACS Appl. Mater. Interfaces 6 (2014) 7996–8000.
[31] L.A. Ridnour, J.E. Sim, M.A. Hayward, D.A. Wink, S.M. Martin, G.R. Buettner, D.R. Spitz, Anal. Biochem. 281 (2000) 223–229.
[32] P.A. Panchenko, A.N. Arkhipova, O.A. Fedorova, Y.V. Fedorov, M.A. Zakharko, D.E. Arkhipov, G. Jonusauskas, Phys. Chem. Chem. Phys. 19 (2017) 1244–1256.
[33] M. Fernández-Marcos, L. Sanz, D.R. Lewis, G.K. Muday, O. Lorenzo, Proc. Natl. Acad. Sci. U.S.A. 108 (2011) 18506.
[34] S. Bai, T. Yao, M. Li, X. Guo, Y. Zhang, S. Zhu, Y. He, Mol. Plant 7 (2014) 616–625.
[35] M. Rico-Lemus, B. Rodríguez-Garay, J. Plant Biochem. Physiol. 2 (2014) e127.
[36] C. Stöhr, S. Stremlau, J. Exp. Bot. 57 (2006) 463–470.